

Complete next-to-leading order calculation for pion production in nucleon-nucleon collisions at threshold

C. Hanhart ^a and N. Kaiser ^b

*a: Forschungszentrum Jülich, Institut für Kernphysik (Theorie)
D-52425 Jülich, Germany*

*b: Institut für Theoretische Physik, Physik-Department T39,
Technische Universität München, D-85747 Garching, Germany*

Abstract

Based on a counting scheme that explicitly takes into account the large momentum $\sqrt{Mm_\pi}$ characteristic for pion production in nucleon-nucleon collisions we calculate all diagrams for the reaction $NN \rightarrow NN\pi$ at threshold up to next-to-leading order. At this order there are no free parameters and the size of the next-to-leading order contributions is in line with the expectation from power counting. The sum of loop corrections at that order vanishes for the process $pp \rightarrow pp\pi^0$ at threshold. The total contribution at next-to-leading order from loop diagrams that include the delta degree of freedom vanishes at threshold in both reaction channels $pp \rightarrow pp\pi^0, pn\pi^+$.

The high precision data for the processes $pp \rightarrow pp\pi^0$, $pp \rightarrow pn\pi^+$ and $pp \rightarrow d\pi^+$ in the threshold region [1] have spurred a flurry of theoretical investigations. The first data on neutral pion production were a big surprise because the experimental cross sections turned out to be a factor of five larger than the theoretical predictions based on direct pion production and neutral pion rescattering fixed from on-shell πN data [2, 3]. Subsequently, it was argued that heavy-meson exchanges might be able to remove this discrepancy [4]. On the other hand, it was found [5, 6] that the (model-dependent) off-shell behavior of the full πN T-matrix can also enhance the cross sections near threshold considerably.

Due to their nature as pseudo-Goldstone bosons the dynamics of pions is largely constrained by chiral symmetry. Thus one might hope that effective field theory studies which incorporate these constraints strictly will help to resolve the so far confusing situation. In the literature there are several calculations carried out in the framework of tree-level chiral perturbation theory including the dimension two (single-nucleon) operators for neutral pion production [7, 8, 9, 10] as well as for charged pion production [11, 12]. A common feature of these calculations is that the contributions from the isoscalar pion rescattering interfere destructively with the direct production amplitude, thus leading to an even more severe discrepancy between experiment and theory. It should be noted that such an interference pattern is in contradiction to the one found in phenomenological approaches [5, 6]. Furthermore, within the Weinberg scheme, where all momenta are considered of the order of m_π , one loop calculations have been performed for neutral pion production $pp \rightarrow pp\pi^0$ [13, 14, 15]. According to some of these works the loop corrections are larger by at least a factor of two compared to the tree level diagrams, that

according to the counting scheme applied appear one order down. This feature (if correct) would seriously question the convergence of the chiral expansion for pion production in NN-collisions. On the other hand, according to ref.[16] the chiral expansion seems to show convergence in the case of p-wave pion production.

The purpose of the present work is to present a complete next-to-leading order calculation of the reaction $NN \rightarrow NN\pi$ at threshold. In particular, we evaluate all one-loop diagrams at next-to-leading order employing a counting scheme that takes into account the large momentum $\sqrt{Mm_\pi}$ characteristic for pion production in NN-collisions, as suggested in refs. [8, 16]. We consider also the contributions from explicit delta-isobars at tree level and at one-loop order. To the order we are working there are no free parameters and we demonstrate that the size of the individual next-to-leading order contributions is in line with the expectations from power counting.

Let us begin with writing down the general form of the threshold T-matrix for the pion production reaction $N_1(\vec{p}) + N_2(-\vec{p}) \rightarrow N + N + \pi$ in the center-of-mass frame, which reads [17]:

$$T_{th}^{cm}(NN \rightarrow NN\pi) = \frac{\mathcal{A}}{2} (i\vec{\sigma}_1 - i\vec{\sigma}_2 + \vec{\sigma}_1 \times \vec{\sigma}_2) \cdot \vec{p} (\vec{\tau}_1 + \vec{\tau}_2) \cdot \vec{\phi}^* + \frac{\mathcal{B}}{2} (\vec{\sigma}_1 + \vec{\sigma}_2) \cdot \vec{p} (i\vec{\tau}_1 - i\vec{\tau}_2 + \vec{\tau}_1 \times \vec{\tau}_2) \cdot \vec{\phi}^*, \quad (1)$$

with $\vec{\sigma}_{1,2}$ and $\vec{\tau}_{1,2}$ the spin and isospin operators of the two nucleons. $\vec{\phi}$ denotes the three-component isospin wave function of the final state pion produced in an s-wave state, e.g. $\vec{\phi} = (0, 0, 1)$ for π^0 -production and $\vec{\phi} = (1, i, 0)/\sqrt{2}$ for π^+ -production. The complex amplitudes \mathcal{A} and \mathcal{B} belong to the transitions ${}^3P_0 \rightarrow {}^1S_0$ and ${}^3P_1 \rightarrow {}^3S_1$ in the two-nucleon system, respectively. In fact the selection rules which follow from the conservation of parity, angular momentum and isospin allow only for these two transitions for the reaction $NN \rightarrow NN\pi$ at threshold. In the case of neutral pion production $pp \rightarrow pp\pi^0$ the threshold amplitude \mathcal{A} is the only relevant one whereas in charged pion production $pp \rightarrow pn\pi^+$ both threshold amplitudes \mathcal{A} and \mathcal{B} can contribute. Note that the threshold T-matrix written in eq.(1) incorporates the Pauli exclusion principle since combined left multiplication with the spin-exchange operator $(1 + \vec{\sigma}_1 \cdot \vec{\sigma}_2)/2$ and the isospin exchange operator $(1 + \vec{\tau}_1 \cdot \vec{\tau}_2)/2$ reproduces $T_{th}^{cm}(NN \rightarrow NN\pi)$ up to an important minus sign. The magnitude of the nucleon center-of-mass momentum \vec{p} necessary to produce a pion at rest is given by:

$$|\vec{p}| = \sqrt{m_\pi(M + m_\pi/4)}, \quad (2)$$

with $M = 939$ MeV and $m_\pi = 139.6$ MeV denoting the nucleon and pion mass, respectively. Eq.(2) exhibits the important feature of the reaction $NN \rightarrow NN\pi$, namely the large momentum mismatch between the initial and the final nucleon-nucleon state. This leads to a large invariant (squared) momentum transfer $t = -Mm_\pi$ between in- and outgoing nucleons. The appearance of the large momentum scale $\sqrt{Mm_\pi}$ in pion production demands for a change in the chiral power counting rules, as pointed out already in ref.[8]. In addition, it seems compulsory to include the delta-isobar as an explicit degree of freedom, since the delta-nucleon mass difference $\Delta = 293$ MeV is comparable to the external momentum $p \simeq \sqrt{Mm_\pi} = 362$ MeV. The hierarchy of scales

$$M \gg p \simeq \Delta \gg m_\pi, \quad (3)$$

suggested by this feature is in line with findings within meson exchange models where the delta-isobar gives significant contributions even close to the threshold [18, 19].

Let us now state our counting rules. The external momentum $p \simeq \sqrt{Mm_\pi}$ sets the overall scale relevant for the process $NN \rightarrow NN\pi$. This momentum scale p enters the internal lines of tree and loop diagrams. Therefore we count all four-momenta^{#1} l_μ inside loops generically as order p and the loop integration measure $\int d^4l$ as order p^4 . A pion propagator is counted as order $1/p^2$. The delta-propagator of the form $1/(\text{energy} - \Delta)$ counts as order $1/p$, since we made the choice $\Delta \sim p$. For the nucleon propagator of the form $1/\text{energy}$ one has to distinguish whether it occurs outside or inside a loop. The associated residual energy counts as order m_π outside a loop and as order $p \sim \sqrt{Mm_\pi}$ inside a loop. Furthermore, external pion energies are counted as order m_π .

According to these counting rules one-loop diagrams contribute at order p^2 in the expansion of the T-matrix and thus generate threshold amplitudes of the form $\mathcal{A}, \mathcal{B} \sim p \simeq \sqrt{Mm_\pi}$. The new counting rules demand also for a reordering of the terms in the interaction Lagrangian, since "relativistic corrections" proportional to nucleon kinetic energies p^2/M are now of the same order as "leading order contributions" proportional to residual nucleon energies. Several examples of this effect will be encountered here.

In Fig. 1, we display tree-level diagrams which according to the abovementioned counting rules contribute at leading order, next-to-leading order and next-to-next-to-leading order. Diagrams for which the role of both nucleons is interchanged and diagrams with crossed outgoing nucleon lines are not shown. Subsets of four diagrams obtained by these operations map properly onto the crossing antisymmetric threshold T-matrix eq.(1). Diagram a) involving the (isovector) Weinberg-Tomozawa $\pi\pi NN$ -contact vertex gives a leading-order contribution of the form:

$$\mathcal{A}^{(WT)} = 0, \quad \mathcal{B}^{(WT)} = -\frac{g_A}{2Mf_\pi^3}, \quad (4)$$

with $g_A \simeq 1.3$ the nucleon axial vector coupling and $f_\pi = 92.4$ MeV the pion decay constant. It is important to note that the Weinberg-Tomozawa vertex generates here a proportionality factor m_π at "leading order" in the chiral πN -Lagrangian via the pion and nucleon (residual) energies as well as through a "relativistic correction" of the form p^2/M . This factor of m_π gets finally canceled by the pion propagator $[m_\pi(M + m_\pi)]^{-1}$. Obviously, the isovector Weinberg-Tomozawa vertex cannot contribute to the neutral pion production threshold amplitude \mathcal{A} . From the one-pion exchange diagram b) one finds:

$$\mathcal{A}^{(1\pi)} = \frac{g_A^3}{8Mf_\pi^3}, \quad \mathcal{B}^{(1\pi)} = \frac{3g_A^3}{8Mf_\pi^3}. \quad (5)$$

This result stems from the recoil correction to the πNN -vertex proportional to $(m_\pi/M) \vec{\sigma}_1 \cdot \vec{p}$ with the m_π -factor getting now canceled by the intermediate nucleon propagator. Furthermore, the product of the two vertices on the left nucleon line $(\vec{\sigma}_1 \cdot \vec{p})^2 = Mm_\pi$ is canceled by the pion propagator. The ratio $\mathcal{B}^{(1\pi)}/\mathcal{A}^{(1\pi)} = 3$ has its origin in the isospin factor of diagram b). From the analogous diagram d) with one virtual delta-isobar excitation one finds:

$$\mathcal{A}^{(\Delta)} = \frac{g_A^3 m_\pi}{4Mf_\pi^3 \Delta}, \quad \mathcal{B}^{(\Delta)} = 0, \quad (6)$$

where we have used the empirically well satisfied relation $h_A = 3g_A/\sqrt{2}$ for the $\pi N\Delta$ -coupling constant. The spin and isospin transition operators entering the $\pi N\Delta$ -vertex $(h_A/2f_\pi) \vec{S} \cdot \vec{p} T_a$

^{#1}Baryon energies are residual energies with the nucleon mass M subtracted.

satisfy the usual relations $S_i S_j^\dagger = (2\delta_{ij} - i\epsilon_{ijk}\sigma_k)/3$ and $T_a T_b^\dagger = (2\delta_{ab} - i\epsilon_{abc}\tau_c)/3$. The latter isospin relation is the reason behind the vanishing of $\mathcal{B}^{(\Delta)}$. According to our counting of the mass-splitting Δ the term $\mathcal{A}^{(\Delta)}$ in eq.(6) is a next-to-leading order contribution, since $\Delta \sim p$ (c.f. relation (3)). Diagram f) involves the second order chiral $\pi\pi NN$ -contact vertex proportional to the low-energy constants $c_{1,2,3,4}$ [20]. We find the following contributions to the threshold amplitudes at next-to-next-to-leading order:

$$\mathcal{A}^{(c_i)} = \frac{g_A m_\pi}{2M f_\pi^3} (c_3 + 2c_2 - 4c_1), \quad \mathcal{B}^{(c_i)} = \frac{g_A m_\pi}{2M f_\pi^3} (c_4 + c_3 + 2c_2 - 4c_1). \quad (7)$$

In a previous calculation in ref.[7] (see eq.(32) therein) the c_2 -term has been found with a relative factor 1/2 smaller. The reason for this discrepancy is again that "relativistic corrections" from the c_2 -vertex are of the same order as its "static" contribution, since $p^2/M = m_\pi$. We also note that our results eqs.(4-7) agree up to the respective order with those of the fully relativistic calculation in ref.[17] where no approximations to the threshold kinematics have been made. We do not specify here the contributions from diagrams c), e) and g) in Fig.1 which are proportional to the (a priori unknown) strengths of four-nucleon contact-vertices etc. It is important to note that already at leading order long-range effects from pion-exchange and short-range contributions appear simultaneously.

Let us now turn to the non-vanishing one-loop diagrams at threshold. Not every loop diagram appearing formally at next-to-leading order truly contributes at that order. In case of the diagrams b) and c) in Fig.2 the (spin-independent) one-loop πN -scattering subdiagrams are proportional to m_π^3 , and this pushes their contributions to the threshold T-matrix eq.(1) beyond next-to-leading order. A closer inspection of diagrams a) in Fig.2 reveals that they contribute in the form $m_\pi \ln m_\pi$ to the threshold amplitudes \mathcal{A} and \mathcal{B} , i.e. beyond next-to-leading order. The specific vertex structures of diagrams d) and e) in Fig.2 make also their next-to-leading order contributions vanishing. Therefore we have to focus only on the diagrams shown in Figs.3 and 4.

We evaluate only the genuine next-to-leading order pieces of the loop integrals emerging from the diagrams in Figs.3 and 4. For instance, in the integrands we can systematically drop terms of order m_π compared to l_0 (and Δ). Straightforward but tedious evaluation leads to the following next-to-leading order contributions of the one-loop diagrams in Fig.3 with nucleons only:

$$\mathcal{A}^{(N-loop)} = \frac{g_A^3 \sqrt{M m_\pi}}{256 f_\pi^5} (-2 - 1 + 3), \quad \mathcal{B}^{(N-loop)} = \frac{g_A^3 \sqrt{M m_\pi}}{256 f_\pi^5} (-2 + 0 + 3). \quad (8)$$

Here, the numerical entries correspond to the diagrams a), b) and c), in that order. Interestingly, the total next-to-leading order loop contribution vanishes identically for neutral pion production $\mathcal{A}^{(N-loop)} = 0$. Diagrams a) and c) in Fig.3 have been calculated fully relativistically (i.e. without any approximation to the threshold kinematics) for $pp \rightarrow pp\pi^0$ in ref.[17]. It is an important check for our calculation that the non-analytical piece proportional to $\sqrt{M m_\pi}$ agrees with the one derived by expanding eq.(16) in ref.[17]. In addition, after correcting a sign error in ref.[14] and extracting at threshold the truly next-to-leading order pieces from that work our results agree with theirs [21].

Numerically, the loop correction in eq.(8) gives $\mathcal{B}^{(N-loop)} = g_A^3 \sqrt{M m_\pi} / 256 f_\pi^5 \simeq 0.70 \text{ fm}^4$. This is about 50% of the leading order one-pion exchange contributions $|\mathcal{B}^{(WT)}| \simeq 1.33 \text{ fm}^4$ or $\mathcal{B}^{(1\pi)} \simeq 1.69 \text{ fm}^4$. Indeed from chiral power counting one expects a similar suppression factor $p/M = \sqrt{m_\pi/M} \simeq 0.4$.

According to our counting of the mass difference $\Delta \sim \sqrt{Mm_\pi}$ loop diagrams with explicit delta-isobars are of the same order as those with nucleons only, namely of order p^2 . The relevant one-loop diagrams which generate truly next-to-leading order contributions are shown in Fig. 4. Straightforward but tedious evaluation leads to the following result:

$$\mathcal{A}^{(\Delta\text{-loop})} = \frac{g_A^3 K(\Delta)}{32f_\pi^5} (8 - 12 + 1 + 3), \quad \mathcal{B}^{(\Delta\text{-loop})} = \frac{g_A^3 K(\Delta)}{32f_\pi^5} (8 - 12 + 3 + 1) \quad (9)$$

with the numerical entries corresponding to the subclasses a), b), c) and d), in that order. The relevant combination of loop functions reads:

$$K(\Delta) = 2J_0(-\Delta) - 2\Delta I_0(-Mm_\pi) + (2\Delta^2 - Mm_\pi) \gamma_0(-\Delta, -Mm_\pi), \quad (10)$$

with the following loop integrals [20] truncated at lowest order according to our counting scheme:

$$J_0(-\Delta) = 4\Delta L(\lambda) + \frac{\Delta}{4\pi^2} \left(\ln \frac{2\Delta}{\lambda} - \frac{1}{2} \right) \sim \mathcal{O}(p), \quad (11)$$

$$I_0(-Mm_\pi) = -2L(\lambda) - \frac{1}{16\pi^2} \left(1 + \ln \frac{Mm_\pi}{\lambda^2} \right) \sim \mathcal{O}(p^0), \quad (12)$$

$$\gamma_0(-\Delta, -Mm_\pi) = \frac{1}{4\pi^2 \sqrt{Mm_\pi}} \int_0^\infty \frac{dx}{1+x^2} \arctan \frac{x\sqrt{Mm_\pi}}{2\Delta} \sim \mathcal{O}(p^{-1}). \quad (13)$$

The (scale dependent) quantity:

$$L(\lambda) = \frac{\lambda^{d-4}}{16\pi^2} \left[\frac{1}{d-4} + \frac{1}{2} (\gamma_E - 1 - \ln 4\pi) \right], \quad (14)$$

denotes for the standard divergent piece in dimensional regularization. The reason for grouping together the three specific diagrams into subclass b) is that this way the (in the chiral limit) singular term $\Delta^2 J_0(-\Delta)/Mm_\pi$ does not appear explicitly. Evidently, the formal limit $\Delta \rightarrow 0$ corresponds to loops diagrams with nucleons only, and therefore $K(0) = -\sqrt{Mm_\pi}/16$ enters eq.(8). Note, however, that for planar box diagrams this limit becomes inconsistent with the counting scheme employed.

One concludes that the contributions stemming from loop diagrams with delta-excitation vanish identically for both threshold amplitudes \mathcal{A} and \mathcal{B} , respectively for both reaction channels $pp \rightarrow pp\pi^0, pn\pi^+$. The complete cancellations in eq.(9) are actually important consistency checks for our power counting scheme $\Delta \sim p$. The combination of loop functions $K(\Delta) \sim p$ in eq.(10) is divergent, but at next-to-leading order there is no local counter term to absorb divergences.

In summary, we have performed here a complete next-to-leading order calculation of the reaction $NN \rightarrow NN\pi$ at threshold. We have employed the counting scheme developed in refs. [8, 16], that explicitly accounts for the large momentum $p \simeq \sqrt{Mm_\pi}$ characteristic for this process. We find that the total next-to-leading order loop corrections either vanish or are in accordance with the expectation from power counting. At this stage we conclude, that the chiral expansion seems to converge also in the s-wave. Note, however, that at next-to-next-to-leading order a large number of loops enters, that have not yet been evaluated completely.

In order to compare our results directly to pion production data the emerging chiral operators have to be folded with (realistic) NN-wave functions. This convolution has been carried out in ref.[15] in a way that the symmetries are preserved. However, in that work the traditional

Weinberg counting has been used. Consequently the results presented in ref.[15] do not allow any firm conclusion about the convergence of the chiral series, since contributions of different orders are mixed and the next-to-next-to-leading order is incomplete. Based on our counting scheme a complete next-to-next-to-leading order calculation is within reach and should be performed. Another direction should be the calculation of loop corrections to the higher partial waves amplitudes.

References

- [1] For a recent review see: H. Machner and J. Haidenbauer, *J. Phys.* **G25** (1999) R231.
- [2] G.A. Miller and P. Sauer, *Phys. Rev.* **C44** (1991) 1725.
- [3] J.A. Niskanen, *Phys. Lett.* **B289** (1992) 227.
- [4] T.-S.H. Lee and D.O. Riska, *Phys. Rev. Lett.* **70** (1993) 2237.
- [5] E. Hernandez and E. Oset, *Phys. Lett.* **B350** (1995) 158.
- [6] C. Hanhart, J. Haidenbauer, A. Reuber, C. Schütz and J. Speth, *Phys. Lett.* **B358** (1995) 21.
- [7] B.Y. Park, F. Myhrer, J.R. Morones, T. Meissner and K. Kubodera, *Phys. Rev.* **C53** (1996) 1519.
- [8] T.D. Cohen, J.L. Friar, G.A. Miller and U. van Kolck, *Phys. Rev.* **C53** (1996) 2661.
- [9] U. van Kolck, G.A. Miller and D.O. Riska, *Phys. Lett.* **B388** (1996) 679.
- [10] T. Sato, T.-S.H. Lee, F. Myhrer and K. Kubodera, *Phys. Rev.* **C56** (1997) 1246.
- [11] C. Hanhart et al., *Phys. Lett.* **B424** (1998) 8.
- [12] C. da Rocha, G.A. Miller and U. van Kolck, *Phys. Rev.* **C61** (2000) 034613.
- [13] E. Gedalin, A. Moalem and L. Razdolskaya, *Phys. Rev.* **C60** (1999) 31.
- [14] V. Dmitrasinovic, K. Kubodera, F. Myhrer and T. Sato, *Phys. Lett.* **B 465** (1999) 43.
- [15] S. Ando, T.S. Park and D.P. Min, *Phys. Lett.* **B 509** (2001) 253.
- [16] C. Hanhart, U. van Kolck and G.A. Miller, *Phys. Rev. Lett.* **85** (2000) 2905.
- [17] V. Bernard, N. Kaiser and Ulf-G. Meißner, *Eur. Phys. J.* **A4** (1999) 259.
- [18] J.A. Niskanen, *Phys. Rev.* **C53** (1996) 526.
- [19] C. Hanhart, J. Haidenbauer, O. Krehl and J. Speth, *Phys. Lett.* **B444** (1998) 25.
- [20] V. Bernard, N. Kaiser and Ulf-G. Meißner, *Int. J. Mod. Phys.* **E4** (1995) 193.
- [21] F. Myhrer, private communications.

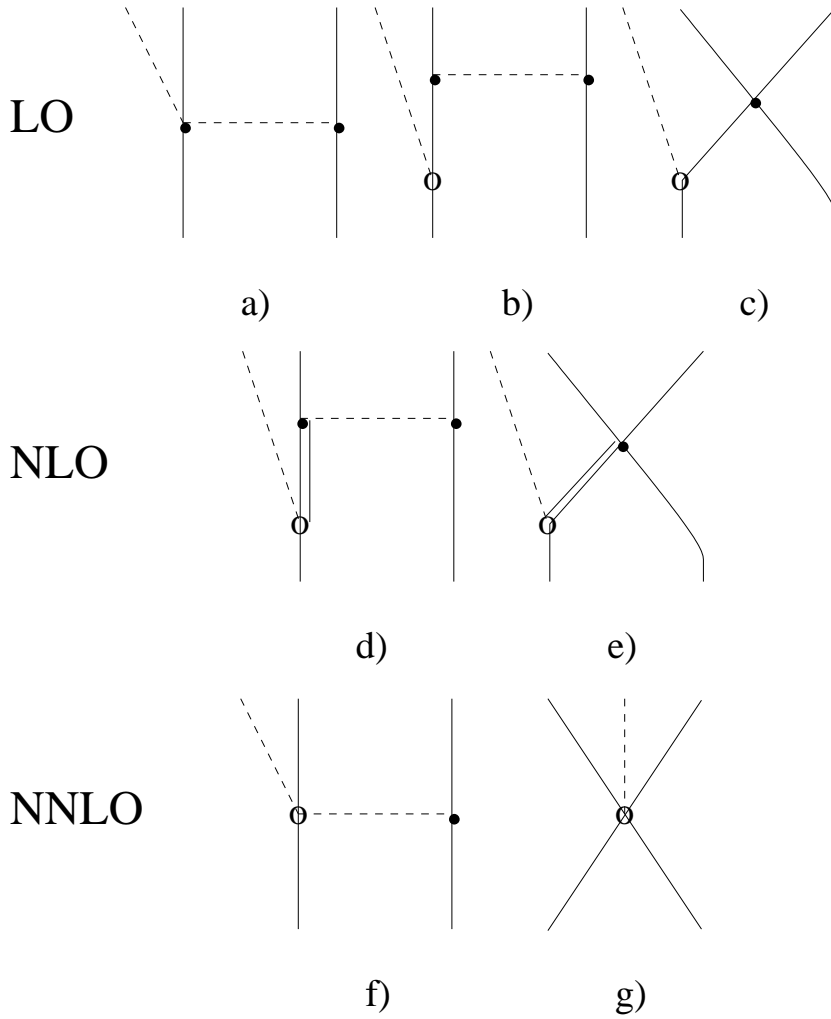


Figure 1: Tree level contributions to threshold pion production at leading order (a,b,c), next-to-leading order (d,e) and next-to-next-to-leading order (f,g). A single solid, double solid and dashed line denotes a nucleon, delta-isobar and pion, respectively. Leading (subleading) order vertices are symbolized by solid dots (open circles).

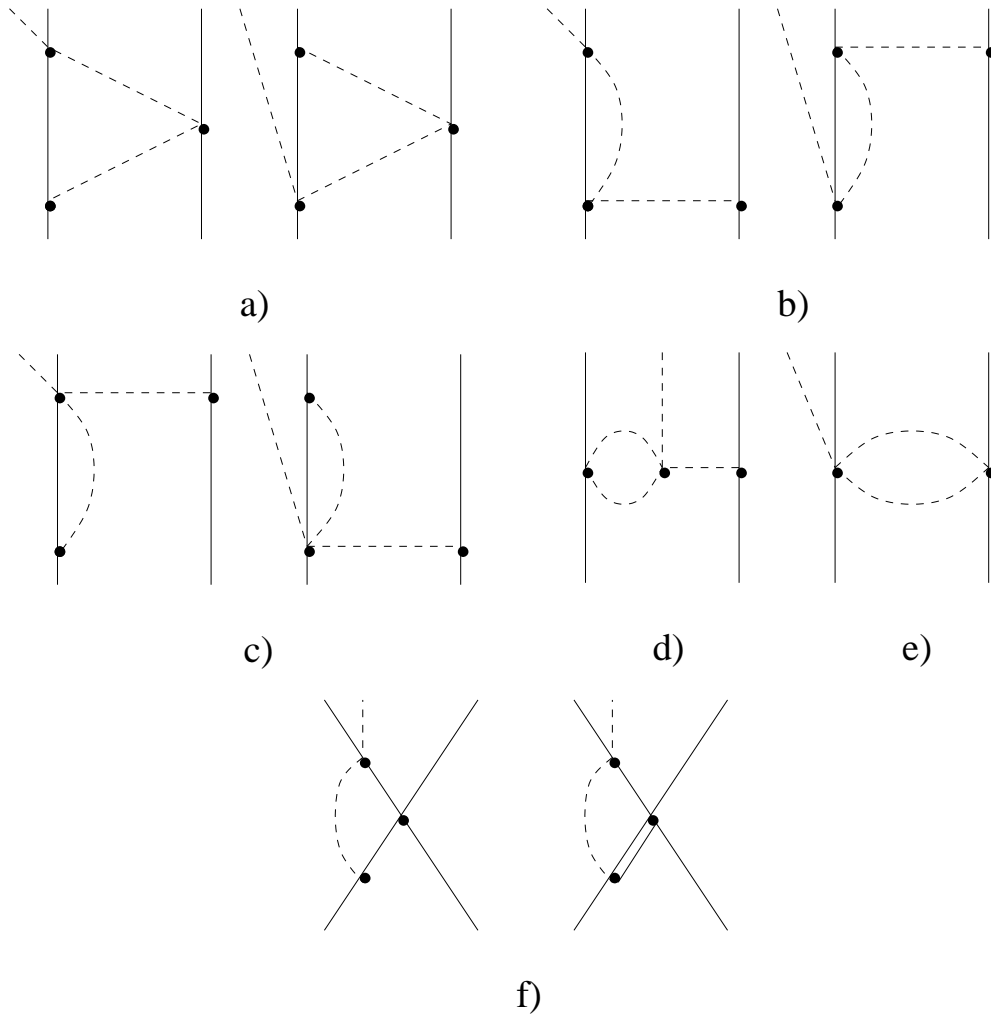


Figure 2: One-loop diagrams that start to contribute at next-to-next-to-leading order. For further notations see Fig. 1.

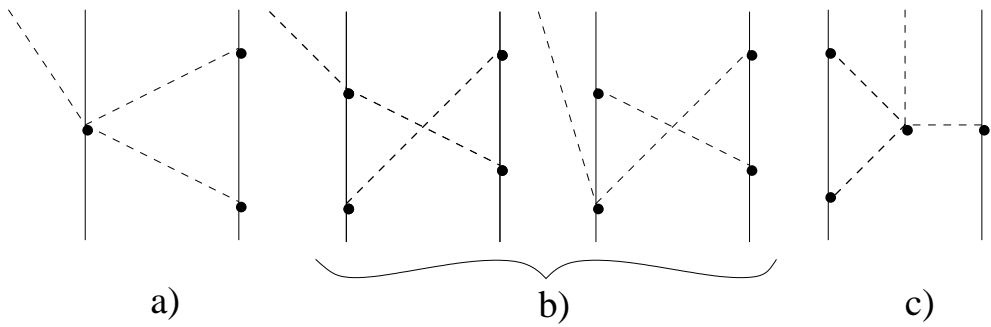


Figure 3: Next-to-leading order one-loop diagrams for pion production at threshold with nucleons only. For further notations see Fig. 1.

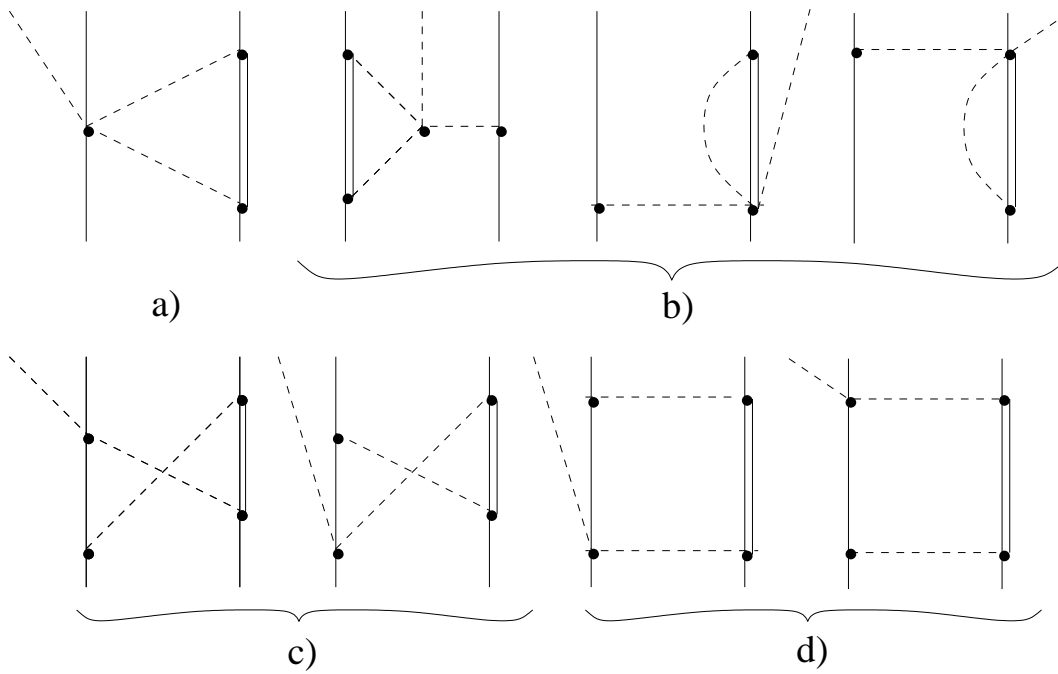


Figure 4: Next-to-leading order one-loop diagrams for pion production at threshold with intermediate delta-isobars. For further notations see Fig. 1.